ISSN (Print) : 0974-6846
ISSN (Online) : 0974-5645
Indian Journal of Science and Technology, *Vol 11(17), DOI: 10.17485/ijst/2018/v11i17/120413, May 2018*

Synthesis, Characterization, Molecular Structures and Anticancer Activity Studies 2-Furan-2-Ylmethyleneamino-Phenyl-Iminomethylphenolcomplexes

Sharah A. A. Aldulmani[1] and Abdel-Nasser M.A. Alaghaz[2,3]

[1]Department of Chemistry, faculty of science for girls, King Khalid University, ABHA, Saudi Arabia;
saldolmani@kku.edu.sa
[2]Department of Chemistry, Faculty of Science, Jazan University, Jazan, Saudi Arabia
[3]Department of Chemistry, Faculty of Science (Boys), Al-Azhar University, Cairo, Egypt;
aalajhaz@hotmail.com

Abstract

Objectives: To synthesize 2-furan-2-ylmethyleneamino-phenyl-iminomethylphenoland its complexes and evaluate the anticancer activity of the ligand and complexes against breast cancer cells. **Methods/Statistical Analysis**: A novel compounds have been synthesized and characterized by many spectral and DFT measurements. The molecular structural parameters of the synthesized furan-Schiff base ligand HL ligand and its isolated metal(II) complexes have been calculated. Anticancer activity for the ligand and the complexes were evaluated against breast cancer cells by using MTT assay. **Findings:** The microanalytical data of the isolated compounds are in good agreement with the calculated values and the spectroscopic analysis of the isolated complexes indicated that the HL ligand coordinated to the metal centers as tetra dentate ligand and form octahedral arrangement around metal(II) centers. The molecular parameters of the ligand and its metal complexes have been calculated and correlated with the experimental data such as IR and TGA results. The results of cells MCF7 breast cancer revealed of cell proliferation was much more highly inhibited by the HL ligand and its isolated complexes Co(II), Ni(II), Cu(II) and Zn(II) with cell viability 24.82, 58.9, 62.7, 73.8 and 87.3%, respectively at a concentration of 1000 PPM compared to untreated control cells. **Application/Improvements:** Lastly, some suggestions were presented to use these isolated compounds in vivo should be assessed to obtain worthy anticancer drugs.

Keywords: Anticancer Activity, Characterization, Isolated Complexes, Molecular Structures, IR, TGA

1. Introduction

Azomethine Schiff neither base ligands containing more than one do nor are sites extensively used for the preparation of metal ion complexes with interesting properties. Transition metal (II/III/IV) complexes of these ligands containing pyridine, furan rings and their derivatives are also of great interest due to their ability to absorb visible light to act as electron reservoirs are promising factors in their applications as photosensitizers[1–3]. Azomethine (CH=N) Schiff bases are considered to be the most important legends in coordination chemistry. They are used as catalysts, dyes and pigments, intermediates in organic synthesis and as polymer stabilizers[4]. Furthermore, azomethine (CH=N) Schiff bases have been utilized in the synthesis of a number of industrial and biologically active compounds such as formazans, benzoxazines, and so on[5]. Azomethine (CH=N) Schiff bases and their complexes have attracted a great interest because of their diverse applications including antimicrobial[6], anticancer[7], anti-oxidant[8], anti inflammatory[9], antiviral[10] and herbicidal[11] activities. Also, some metal complexes of azomethine (CH=N) Schiffbases have been utilized as model molecules for biological oxygen carrier systems[12] as well as possessing analytical applications[13]. Currently, a great interest is being focused on polydentate azomethine (CH=N) Schiffbases. This is due to their ability to form varieties of complexes with various stoichiometry, chelating, magnetic and spectral properties[14]. There is a significant interest to synthesize and characterize metal complexes with bicompartmental ligands[15]. This is due to their importance in biomimetic researches of binuclear metalloproteins[16], their interesting catalytic properties as well as their capability to stabilize unusual oxidation states and mixed valence compounds. In our present work, novel metal(II) complexes were discussed using different studding techniques such as elemental analyses, molar conductance, magnetic moment, and UV–Vis., IR, ^{1}H &^{13}C NMR, mass, EPR, XRD,TGA and molecular structure behavior.

2. Experimental

2.1 Characterization

Elemental analyses were carried out on a Perkin–Elmer 2408 CHN Analyzer. The UV-Visible absorption spectra of the samples were recorded on a UV2 Unicam UV/Vis Spectrophotometer. Magnetic moments (μ_{eff}) were calculated with a Sherwood scientific magnetic susceptibility balance at 294 K. The FT-IR spectra analysis was recorded on a Mattson 5000 FTIR Spectrophotometer. The NMR spectra analyses were measured on a Varian-Gemini-200 MHz Spectrophotometer. The molar conductivities were measured on a CON 6000 conductivity meter. Thermal analyses (TG) were obtained out by using a Shimadzu TG-50 Thermal analyzer. Powder X-ray diffraction patterns were recorded with an X-Pert PRO. The molecular modeling calculations were measured by using DMOL^3 program.

2.2 Synthesis of 2-Furan-2-Ylmethyleneamino-Phenyl-Iminomethylphenol (HL)

The new furan-Schiff base ligand HL was prepared by adding benzene 1,2-diamine (0.108 g, 1 mmol), 2-hydroxybenzaldehyde (0.122 g, 1 mmol), and furan-2-carbaldehyde (0.096g, 1 mmol) dissolved in dry absolute ethanol (40 ml). The mixture of reaction was heated under reflux for 3 h and a yellow precipitate is formed upon cooling the solution to room temperature. The product was filtered off and washed with few amounts of ethanol then diethyl ether, air-dried and recrystallized from ethanol. The purity of prepared furan-Schiff base ligand was measured by TLC employing silica gel as shown in (Figure 1).

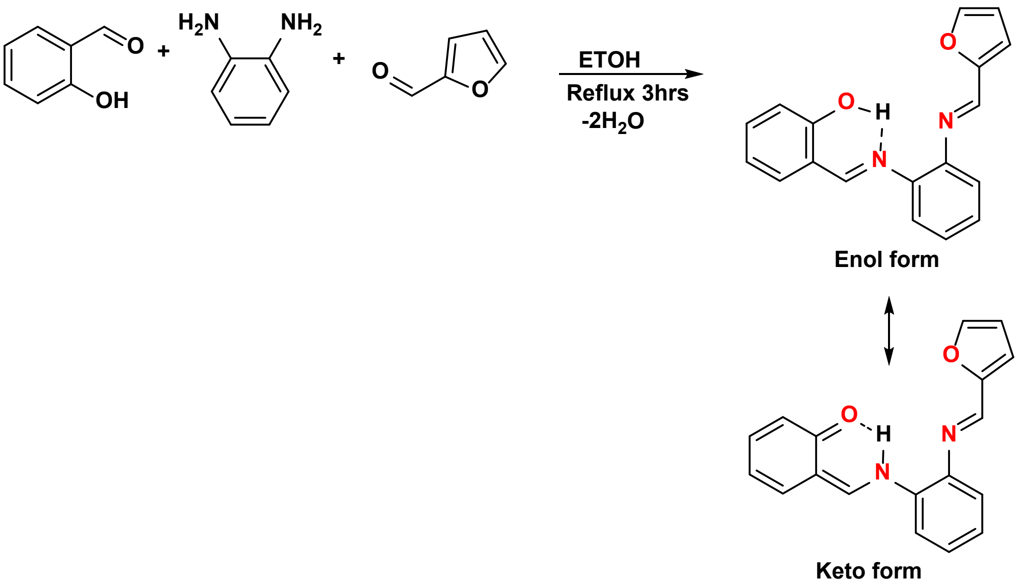

Figure 1. Synthesis and proposed structure of 2-furan-2-ylmethyleneamino-phenyl-iminomethyl-phenol (HL).

2.3 Synthesis of 2-Furan-2-Ylmethyleneamino-Phenyl-Iminomethylphenol Complexes

The new furan Schiff base HL ligand (1 mmol) was dissolved in 10 mL of dichloromethane and then 1 mmol of $CoCl_2.6H_2O$, $NiCl_2.6H_2O$, $CuCl_2.2H_2O$ and $ZnCl_2$ dissolved in 10 mL of ethanol was added drop-wise and the reaction mixture was stirred and heated at 50°C for 4 h. The solvent was allowed to evaporate slowly to produce a solid. The resultant product was collected by filtration and washed with dichloromethane and ethyl acetate to get the pure complex. The physical properties and analytical data of the new furan-Schiff base ligand and its corresponding metal(II) complexes are scheduled in Table 1.

Table 1. Formula, molecular weight, melting point, yield, and elemental analysis data of 2-furan-2-ylmethyleneamino-phenyl-iminomethyl-phenol and its complexes

No.	Compound M.F. (M.Wt.)	Color	M.P. °C	Yield %	Elemental analysis calc. (found)					Λ_m^a
					C	H	N	Cl	M	
Ligand	HL $C_{18}H_{14}N_2O_2$ (290.3)	Orange	142	93	74.47 (74.68)	4.86 (4.73)	9.65 (9.52)	--	—	—
1	$[CoL(H_2O)Cl].2H_2O$ $C_{18}H_{19}ClN_2O_5Co$(437.7)	Olive	>300	86	49.39 (49.39)	4.38 (4.38)	6.40 (6.37)	8.10 (8.04)	13.46 (13.42)	7.32
2	$[NiL(H_2O)Cl].4H_2O$ $C_{18}H_{23}ClN_2O_7Ni$(473.5)	Brown	>300	84	45.66 (45.53)	4.90 (4.88)	5.92 (5.82)	7.49 (7.43)	12.39 (12.34)	9.12
3	$[CuL(H_2O)Cl].3H_2O$ $C_{18}H_{21}ClN_2O_6Cu$ (460.4)	Pale brown	>300	83	46.96 (46.91)	4.60 (4.55)	6.09 (6.02)	7.70 (7.68)	13.80 (13.76)	6.54
4	$[ZnL(H_2O)Cl].5H_2O$ $C_{18}H_{25}ClN_2O_8Zn$(498.2)	Orange	>300	86	43.39 (43.33)	5.06 (5.00)	5.62 (5.57)	7.12 (7.08)	13.12 (13.09)	8.36

a Λ_m = molar conductance ($\Omega^{-1}cm^2mol^{-1}$)

2.4 Anticancer Activities of Ligand and Complexes by using (MTT) Assay

Study of the anticancer activity was by using MTT assay, which is used to evaluate these compounds on viability cancer breast MCF7 Cells. Absorption of the samples was measured by an ELISA reader at 570 nm. Survival fraction was calculated as percentage of the untreated control.

3. Results and Discussions

3.1 Characterization of 2-Furan-2-Ylmethyleneamino-Phenyl-Iminomethyl-Phenol (HL)

The results of micro analytical data of 2-furan-2-ylmethyleneamino-phenyl-iminomethyl-phenolwith Molecular Formula (M.F.) and the Melting Point (m.p.) are recorded in Table 1 & Figure 1. The FT-IR spectrum (Table 2) of 2-furan-2-ylmethyleneamino-phenyl-iminomethyl-phenol is given in synthetic procedures. Vibration bands with the wave numbers of 3364 cm^{-1} (νO–H), 3076 cm^{-1} (νC–H, Ar–H), 1623 cm^{-1} (νCH=N), 1567 cm^{-1} (νC=C), 1214 cm^{-1} (νC–O, Ar–O) was observed for azomethine Schiff base ligand (HL) (Figure 2). The stretching frequency observed at 2853 cm^{-1} in 2-furan-2-ylmethyleneamino-phenyl-iminomethyl-phenol shows the presence of O–H…N intermolecular hydrogen bond. 2-furan-2-ylmethyleneamino-phenyl-iminomethyl-phenol with strong band at 1214 cm^{-1} possesses highest percentage of enolimino tautomer due to the stabilization of phenolic C–O bond. Similarly, the band at 1024 cm^{-1} in 2-furan-2-ylmethyleneamino-phenyl-iminomethyl-phenol coresponds ν(C–O–C) stretching vibration of the furan ring[17]. The ^{1}H NMR data for 2-furan-2-ylmethyleneamino-phenyl-iminomethyl-phenol (Figure 3) shows that the tautomeric equilibrium favors the enol‑imine in DMSO. The broad signal at δ = 11.93ppm is assigned to the proton of the hydroxyl group. This signal is due to hydrogen bonded phenolic proton and the integration is generally less than 2.0 due to this intermolecular hydrogen bonding. Signal for the azomethine (C<u>H</u>=N) proton of the characteristic azomethine group for 2-furan-2-ylmethyleneamino-phenyl-iminomethyl-phenol,–N=C(H)–

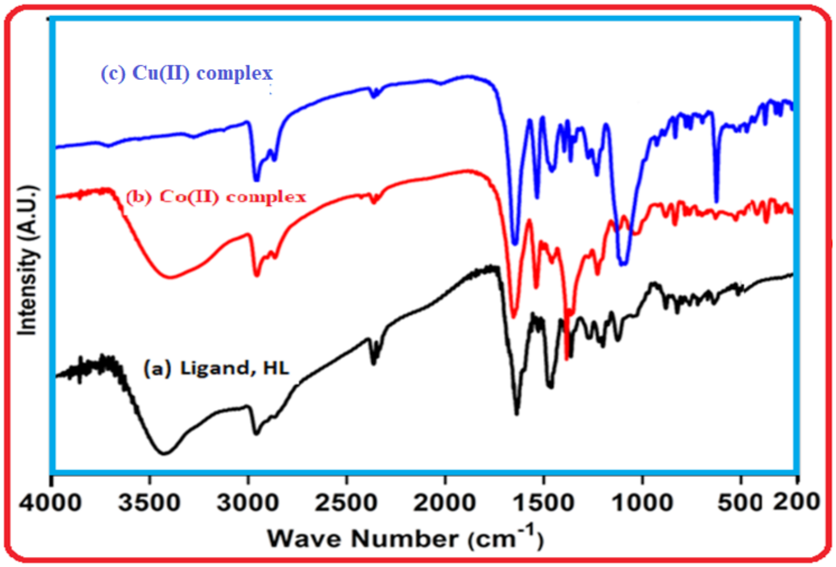

Figure 2. (a) FT-IR spectrum of 2-furan-2-ylmethyleneamino-phenyl-iminomethyl-phenol. (b) FT-IR spectrum of $[Co(L)(H_2O)Cl].2H_2O$ complex and (c) FT-IR spectrum of $[Cu(L)(H_2O)Cl].3H_2O$ complex.

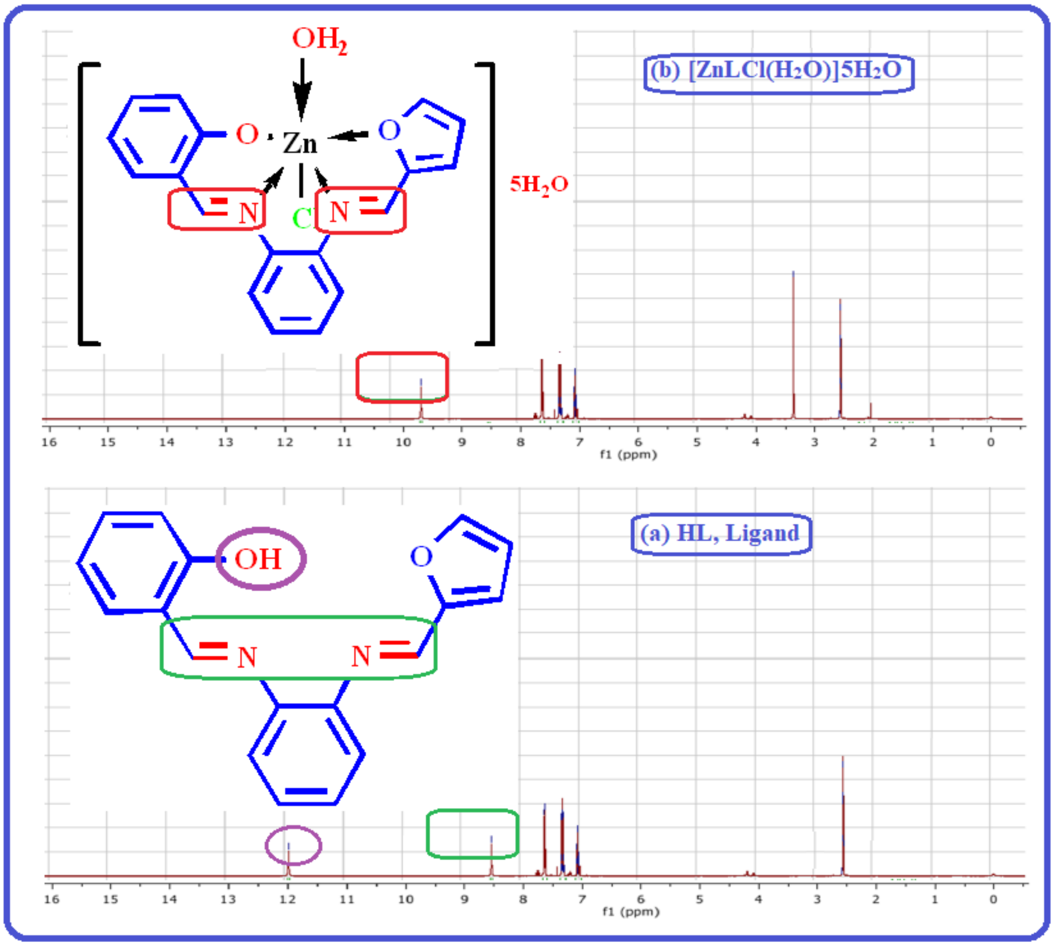

Figure 3. (a) ^1H NMR spectrum of 2-furan-2-ylmethyleneamino-phenyl-iminomethyl-phenol. (b) ^1H NMR spectrum of $[ZnL(H_2O)Cl].5H_2O$ complex.

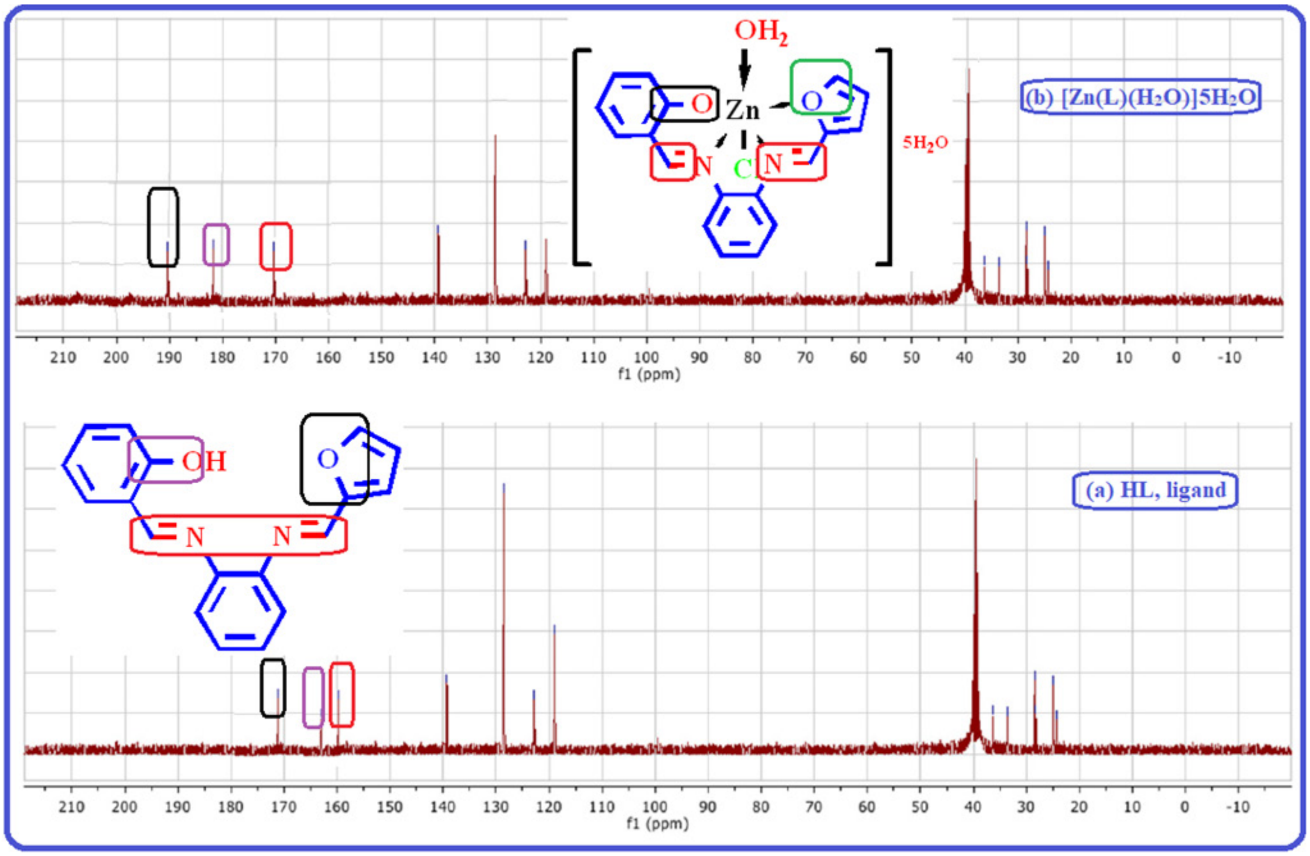

Figure 4. (a) ^{13}C NMR spectrum of 2-furan-2-ylmethyleneamino-phenyl-iminomethyl-phenol. (b) ^{13}C NMR spectrum of $[ZnL(H_2O)Cl].5H_2O$ complex.

Table 2. IR Spectral data (cm^{-1}) of 2-furan-2-ylmethyleneamino-phenyl-iminomethyl-phenol and its metal complexes

Compound	ν_{OH}	$\nu_{(OH)water}$	$\nu_{C=N}$	ν_{C-O}	$\nu_{(C-O-C)furan}$	ν_{M-O}	νM-N	νM-Cl
HL	3364br	–	1623m	1214m	1024m	–	–	–
$[CoL(H_2O)Cl].2H_2O$	–	3318br	1601m	1202m	1008m	376m	355w	262m
$[NiL(H_2O)Cl].4H_2O$	–	3320br	1600m	1200m	1009s	380s	348w	274w
$[CuL(H_2O)Cl].3H_2O$	–	3320br	1601s	1203m	1012m	363m	352m	267m
$[ZnL(H_2O)Cl].5H_2O$	–	3300r	1600m	1203m	1010m	365m	345m	277m

sh = sharp, m = medium, br = broad, s = small, w = weak

was observed at 8.57ppm. In the region of 6.88–7.37 ppm chemical shifts were assigned for hydrogen of the aromatic ring. In ^{13}C NMR of 2-furan-2-ylmethyleneamino-phenyl-iminomethyl-phenol (Figure 4) azomethine carbon at 160.12 ppm. The Ultraviolet spectrum of 2-furan-2-ylmethyleneamino-phenyl-iminomethyl-phenol in ethanol, dichloromethane, acetonitrile and hexane shows absorption bands at 224, 232, 257 and 262 nm are assigned to $\pi \rightarrow \pi^*$ transitions of the enol–imine tautomer of the azomethine furan-Schiff's base HL ligand. The observed small hypsochromic shift of the 332 nm band in more polar solvents is typical to $n \rightarrow \pi^*$ transitions of C=N group. The maximum at 417 nm detected in the EtOH solutions of 2-furan-2-ylmethyleneamino-phenyl-iminomethyl-phenol is assigned to $n \rightarrow \pi^*$ transitions in dipolar zwitterionic or keto–imine tautomeric structures, respectively.

The electron impact mass spectrum (Figure 5) of 2-furan-2-ylmethyleneamino-phenyl-iminomethyl-phenol, confirms the proposed formula by showing a peak at 280 u corresponding to the ligand moiety [$(C_{18}H_{14}N_2O_2)$ atomic mass 290u]. The series of peaks in the range i.e., 5282,118, 148, 152, 208 and 227u, attributable to different fragments of 2-furan-ylmethyleneamino-phenyl-iminomethyl-phenol.

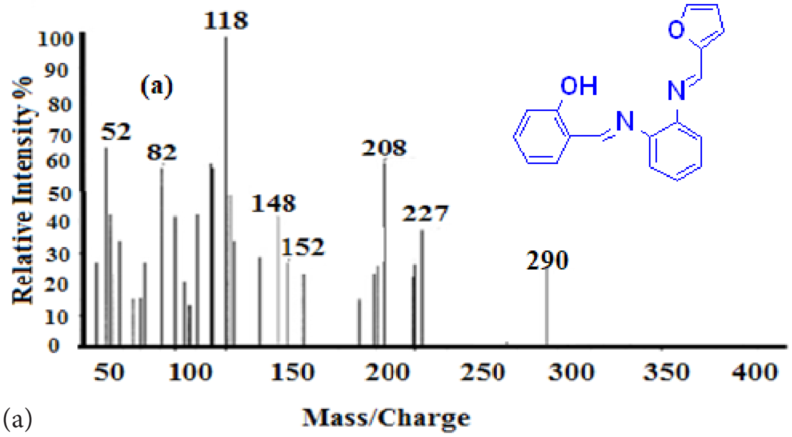

(a)

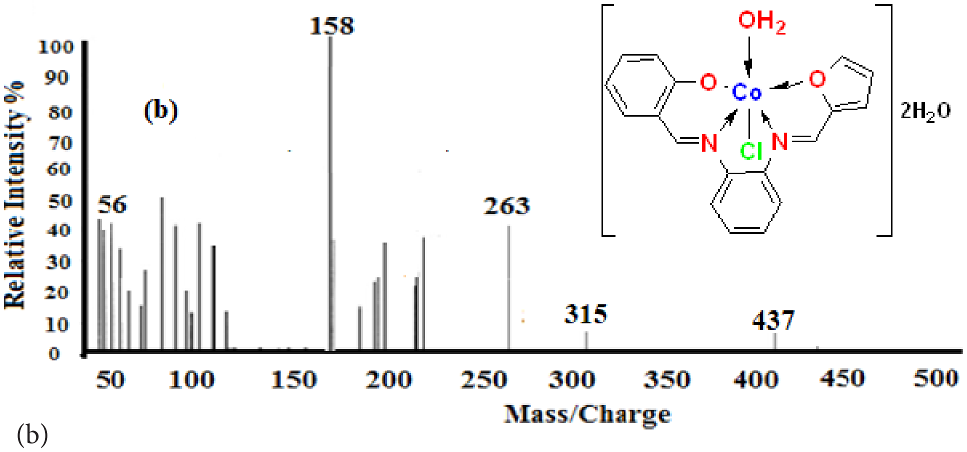

(b)

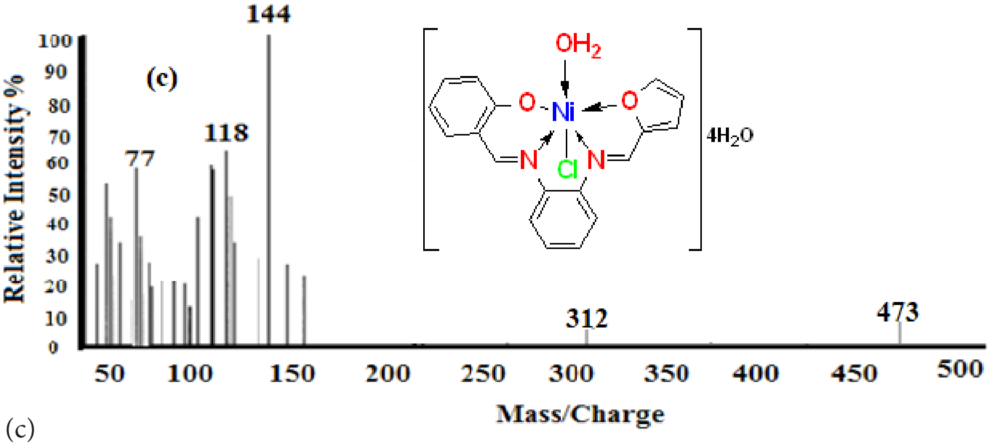

(c)

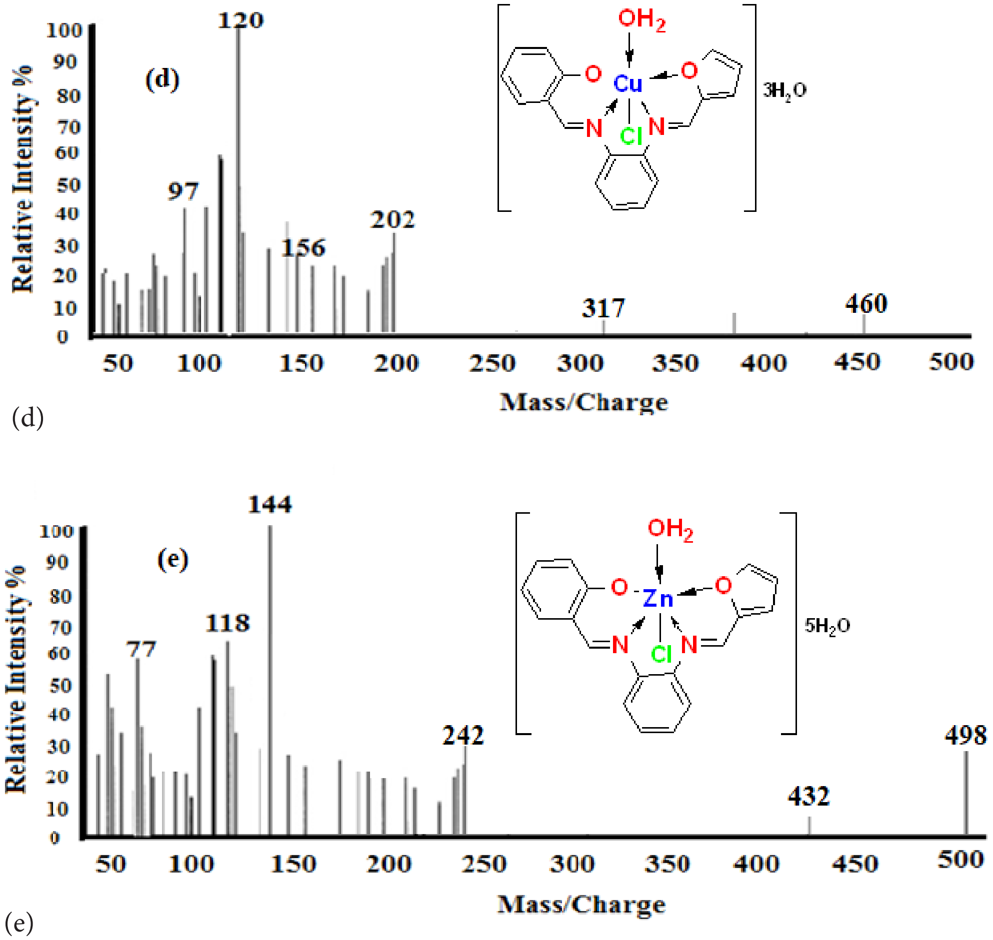

(d)

(e)

Figure 5. Mass spectra of. (a) 2-furan-2-ylmethyleneamino-phenyl-iminomethyl-phenol. (b) $[CoL(H_2O)Cl].2H_2O$ complex. (c) $[NiL(H_2O)Cl].4H_2O$ complex. (d) $[CuL(H_2O)].3H_2O$ complex. (e) $[ZnL(H_2O)].5H_2O$ complex.

3.2 Characterization of 2-Furan-2-Ylmethyleneamino-Phenyl-Iminomethyl-Phenol Metal Complexes

On the basis of analytical data (Table 1), all 2-furan-2-ylmethyleneamino-phenyl-iminomethyl-phenol complexes have the general composition $[ML(H_2O)Cl].nH_2O$ {L = 2-furan-2-ylmethyleneaminophenyl-iminomethyl-phenol and for M = Co(II), n = 2; Ni(II), n = 4; Cu(II) , n = 3; and Zn(II), n = 5}. The Λ_m (molar conductance) of the soluble related 2-furan-2-ylmethyleneamino-phenyl-iminomethyl-phenolcomplexes(1-4) in dimethylformamide showed values in the ranges 6.54–9.12 Ohm^{-1} cm^2 mol^{-1} elucidating that are non-electrolytes in nature[18]. In the IR spectra of 2-furan-2-ylmethyleneamino-phenyl-iminomethyl-phenol complexes (Figure 2, Table 2), the absorption at 1623 cm^{-1} attributed to the presence of azomethine group (–CH=N) and shifting of this band to lower frequency region (by 23 cm^{-1}) in all corresponding 2-furan-2-ylmethyleneamino-phenyl-iminomethyl-phenol complexes indicate the coordination of azomethine nitrogen (–C=N) to metalion and this can be explained by the donation of electrons from nitrogento the empty d–orbital of the metal ion. A broad band at 3364 cm^{-1} is observed due to phenolic-OH group that disappears in the spectra of all furan-Schiff's base metal(II) complexes suggest the deprotonation of phenolic-OH group by metal ion. The band observed at 1214 cm^{-1} are assigned to phenolic C–O stretching vibration, respectively, which get shifted to lower frequency in all corresponding 2-furan-2-ylmethyleneamino-phenyl-iminomethyl-phenol complexes and consistent with coordination via the protonated phenolic oxygen[19]. Also, the specific band of ν(C–O–C) furan ring vibration at 1024 cm^{-1} in ligand shifts to (1008–1012 cm^{-1}) in all 2-furan-2-ylmethyleneamino-phenyl-iminomethyl-phenol complexes[20]. Bands observed in the ranges 380–363, 355–345 and 262–277 may be assignable to (M–O), (M–N) and (M–Cl)[21].

The ^{1}H NMR spectroscopic data of 2-furan-2-ylmethyleneamino-phenyl-iminomethyl-phenol (Figure 3(a)) and its $[ZnL(H_2O)Cl].5H_2O$ complex (Figure 3(b)) have been recorded in DMSO-d6. The broad signal at 11.93 ppm is due to the –OH proton in 2-furan-2-ylmethyleneamino-phenyl-iminomethyl-phenol disappearance of the signal for spectrum of the –OH proton in the spectrum of the $[ZnL(H_2O)].5H_2O$ complex supported the protonation of the thiol group. The signal of the azomethine proton is shifted to high field in the spectrum of $[ZnL(H_2O)Cl].5H_2O$ complex. In^{13} C NMR of 2-furan-2-ylmethyleneamino-phenyl-iminomethyl-phenol (Figure 4a) (–$\underline{\text{C}}$=N–) azomethine carbon showed signal at 160.12 ppm[25], (–$\underline{\text{C}}$–O) phenolic group carbon at 163.27 ppm[22], ($\underline{\text{C}}$–O) furan ring at 170.12[23]. The signals due to (–$\underline{\text{C}}$=N–) azomethine, (–$\underline{\text{C}}$–O) phenolic and ($\underline{\text{C}}$–O) furan carbons were slightly shifted downfield in comparison to the corresponding signals of these groups in the ligand thereby confirming the complexation with zinc metal ion. It was observed that DMSO did not have any coordinating effect on the spectrum of $[ZnL(H_2O)Cl].5H_2O$ complex (Figure 4(b)). The recorded mass spectra of 2-furan-2-ylmethyleneamino-phenyl-iminomethyl-phenol complexes (Figure 5(b-e)) and the molecular ion peaks at 437, 473, 460 and 498 for corresponding furan-Schiff's base metal(II) complexes, have been used to confirm the proposed formula (437, 473, 460 and 498u for Co(II), Ni(II), Cu(II) and Zn(II) complexes, respectively).

The electronic spectrum of the Co(II) complex(Figure 6 and Table 3) records three bands at 10,696, 15,191 and 25,067 cm^{-1} . These bands may be assigned to following transitions $^4T_1g \rightarrow {}^4T_2g(F)$ (v_1), $^4T_1g \rightarrow {}^4A_2g(F)(v_2)$ and $^4T_1g \rightarrow {}^4T_1g(P)$ (v_3), respectively. The position of bands suggests octahedral geometry of Co(II) complex[24]. Co(II) complex shows magnetic moment at 3.98 B.M. corresponding to three unpaired electrons. Ligand field parameters were calculated for the cobalt(II) complex. The value of Dq has been calculated from Orgel energy level diagrams using the v_3/v_1 ratio[24]. The value for *B* (free ion) is 1126 cm^{-1}. The value of β indicates that the covalent character of metal ligand σ-bond is low (Table 4).

Electronic spectrum of Ni(II) complex (Figure 6(b); Table 3) displays bands at 11,357, 15,803 and 21,489 cm^{-1}, these bands may be assigned to $^3A_2g(F) \rightarrow {}^3T_2g(F)$ (ν_1), $^3A_2g(F) \rightarrow {}^3T_1g(F)(\nu_2)$ and $^3A_2g(F) \rightarrow {}^3T_1g(P)(\nu_3)$ transitions, respectively. It suggests octahedral geometry of Ni(II) complex[24]. The nickel(II) complex shows magnetic moment 2.92 B.M. corresponding to two unpaired electrons[24].

Electronic spectrum of the copper(II) complex (Figure 6(c); Table 3) displays bands at 18,534, and 30,373 cm^{-1}. First two bands may be assigned to the transitions: $^2B_1g \rightarrow {}^2A_1g\ (dx^2 - y^2 \rightarrow dz^2)(v_1)$, $^2B_1g \rightarrow {}^2B_2g\ (dx^2 - y^2 \rightarrow dzy)(v_2)$, respectively and third band may be due to charge transfer. The observed magnetic moment of the Cu(II) complex is 1.96 B.M., which confirms the octahedral structure of this complex[25].

The Zn(II) complex (Figure 6(d); Table 3) is diamagnetic as expected and its geometry is most probably octahedral similar to the Cu(II), Co(II) and Ni(II) complexes of the HL ligand.

The solid state ESR spectrum of $[CuL(H_2O)Cl].3H_2O$ complex (Figure 7) is displayed at room temperature. The shape of the spectrum is consistent with octahedral environment around Cu(II) ion and the higher *g* value for the investigated $[CuL(H_2O)Cl].3H_2O$ complex, when compared to that of free electron (g = 2.24) revealing an appreciable covalency of metal ligand bonding with $dx^2 - y^2$ as the ground-state characteristic of octahedral stereochemistry[25]. Also, the $g_{||}/A_{||}$ value 143 for the $[CuL(H_2O)Cl].3H_2O$complex lies just within the range expected for octahedral complex[25]. The decrease of 9 the *g* value than that of the free-electron value (2.07) is an approximate measure of the ligand field strength; the stronger the furan-Schiff's base ligand field the smaller the decrease in the g value and vice versa. The cell parameters (Figure 8, Table 5) of $[CoL(H_2O)Cl].2H_2O$, $[NiL(H_2O)Cl].4H_2O$, $[CuL(H_2O)Cl].3H_2O$ and $[ZnL(H_2O)Cl].5H_2O$ complexes were measured by using XRD powder[26,27] of giving triclinic, monoclinic, orthorhombic and orthorhombic crystal systems, respectively.

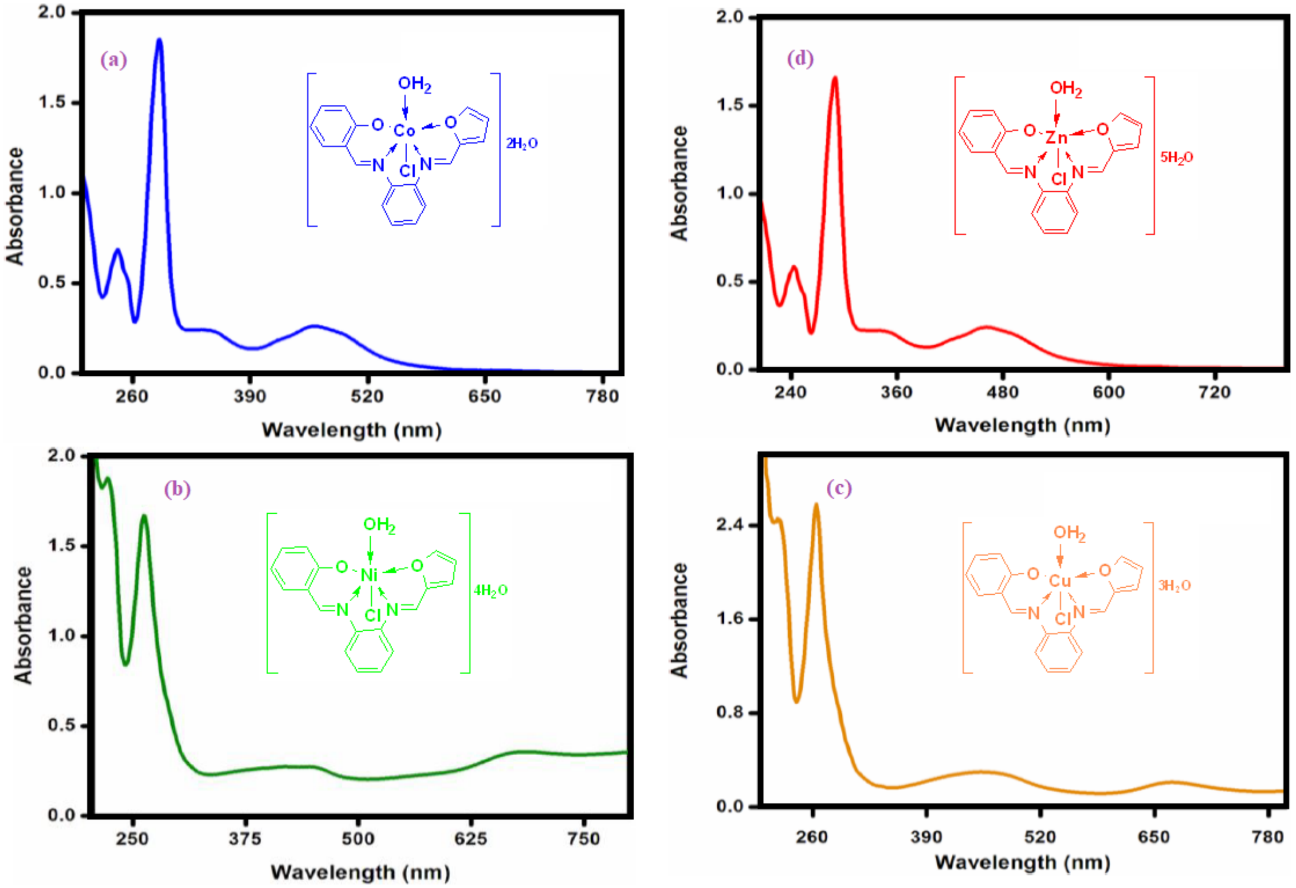

Figure 6. Electronic spectra of. (a) $[CoL(H_2O)Cl].2H_2O$complex. (b) $[NiL(H_2O)Cl].4H_2O$complex. (c) $[CuL(H_2O)].3H_2O$ complex. (d) $[ZnL(H_2O)].5H_2O$ complex.

Table 3. Molar conductance, magnetic moment and electronic spectral data of the complexes

Complex	Geometry	μ_{eff} (B.M.)	Band assignments	λ_{max} (cm^{-1})
$[Co(L)(H_2O)Cl].2H_2O$	Octahedral	3.98	$^4T_1 \rightarrow {}^4T_2(F)\ (\nu_1)$ $^4T_1 \rightarrow {}^4A_2(F)\ (\nu_2)$ $^4T_1 \rightarrow {}^4T_1g(P)\ (\nu_1)$	10,696 15,191 25,067
$[Ni(L)(H_2O)Cl].4H_2O$	Tetrahedral	2.92	$^3A_2(F) \rightarrow {}^3T_2(F)\ (\nu_2)$ $^3A_2(F) \rightarrow {}^3T_1(F)\ (\nu_3)$ $^3A_2(F) \rightarrow {}^3T_1(P)\ (\nu_3)$	11,357 15,803 21,489
$[Cu(L)(H_2O)Cl].3H_2O$	Octahedral	2.06	$^2B_1g \rightarrow {}^2A_1g(dx^2 - y^2 \rightarrow dz^2)(\nu_1)$ $^2B_1g \rightarrow {}^2A_2g(dx^2 - y^2 \rightarrow dzy)(\nu_2)$	18,534 30,373
$[Zn(L)(H_2O)Cl].5H_2O$	Octahedral	diamagnetic	LMCT(M←N)	25,674

Table 4. Ligand field parameters of the complexes

Complex	Dq (cm^{-1})	B(cm^{-1})	β	LFSE ($kJmol^{-1}$)	F_2	F_4	C	ν_2/ν_1
[Co(L)(H2O)Cl].2H2O	1168	808	0.73	100.47	–	–	–	1.42
$[Ni(L)(H_2O)Cl].4H_2O$	792	–	0.95	114.23	–	–	–	1.39
$[Cu(L)(H_2O)Cl].3H_2O$	–	–	–	–	–	–	–	2.00

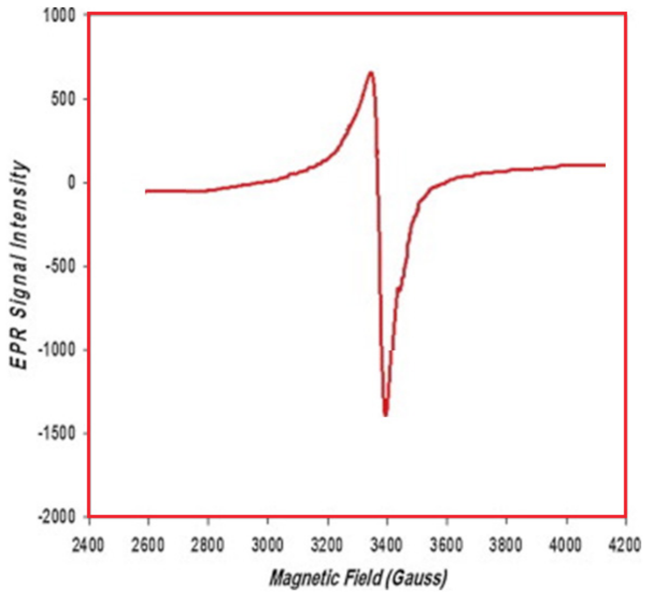

Figure 7. EPR spectrum of $[Cu(L)(OH_2)]3H_2O$ complex.

The stages of decomposition, temperature range, decomposition product as well as the weight loss percentages of 2-furan-2-ylmethyleneamino-phenyl-iminomethyl-phenol and their corresponding metal(II) complexes (1–4) were characterized by Thermogravimetric Analysis (TGA). The TGA curves are given in Figure 9 and the data are listed in Table 6. The weight losses for each compound are calculated within the corresponding temperature ranges.

2-furan-2-ylmethyleneamino-phenyl-iminomethyl-phenol (HL) shows four decomposition steps, the first stage occurs in the temperature range of 50-125°C is attributed to loss of phenol moiety (Found 32.38% and calc. 32.41%). The second stage in the temperature range of 125–205°C corresponding o loss of furan (Found 23.42%, calc. 23.45%). The third stage in the temperature range of 205–395°C corresponding to loss of a part

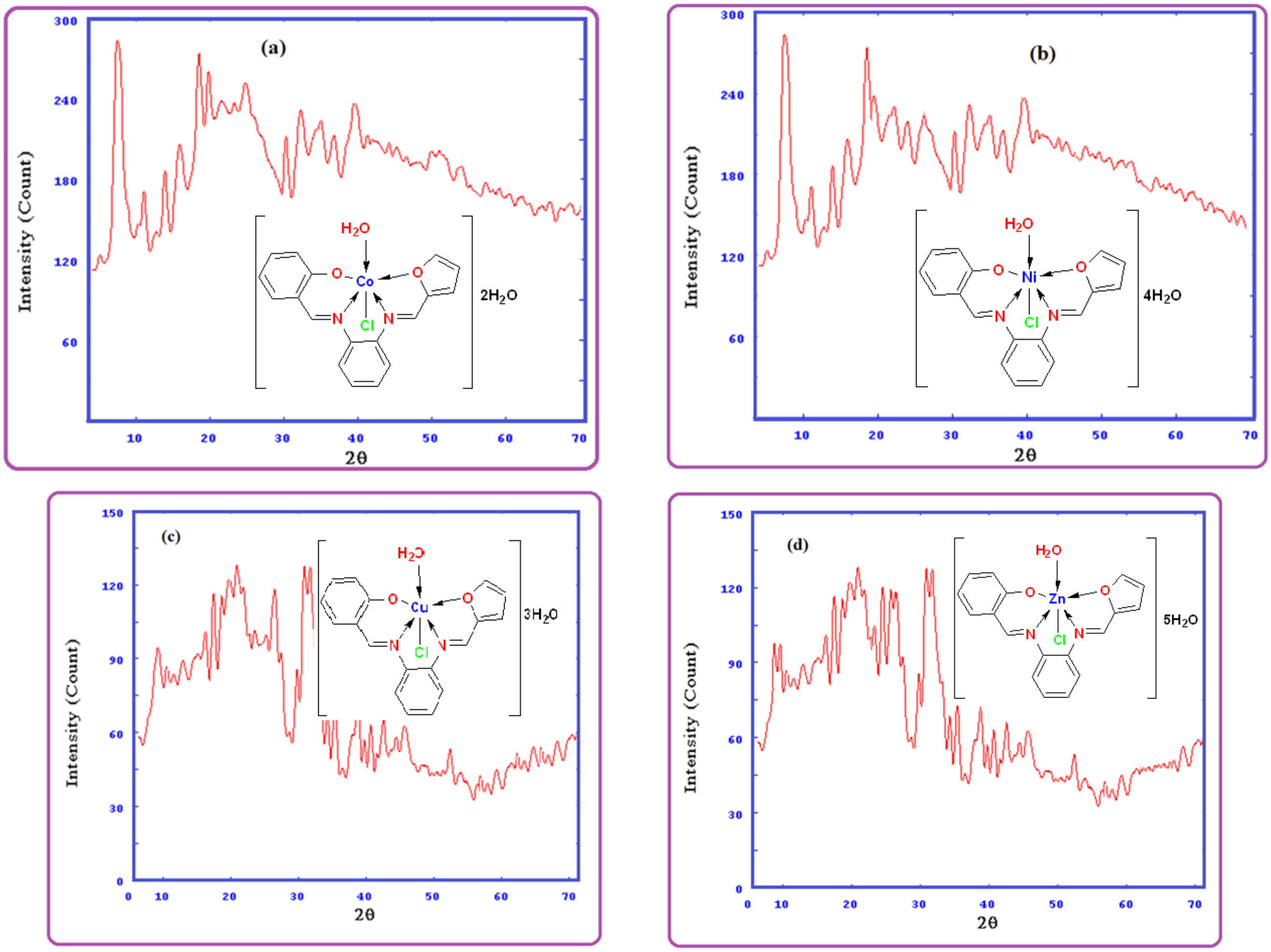

Figure 8. X-ray diffraction pattern of. (a) $[CoLCl(H_2O)].2H_2O$ complex. (b) $[NiLCl(H_2O)].4H_2O$ complex. (c) $[CuLCl(H_2O)].3H_2O$ complex. (d) $[ZnLCl(H_2O)].5H_2O$ complex.

Table 5. Crystallographic data for the Schiff base complexes [CoLCl(H_2O)].2H_2O, [NiLCl(H_2O)].4H_2O, [CuLCl(H_2O)].3H_2O, [ZnLCl(H_2O)].5H_2O

Data	**[CoLCl(H_2O)].2H_2O**	**[NiLCl(H_2O)].4H_2O**	**[CuLCl(H_2O)].3H_2O**	**[ZnLCl(H_2O)].5H_2O**
Empirical formula	$C_{18}H_{19}ClN_2O_5Co$	$C_{18}H_{24}ClN_2O_7Ni$	$C_{18}H_{21}ClN_2O_6Cu$	$C_{18}H_{25}ClN_2O_8Zn$
Formula weight (g/mol)	437.7	473.5	460.4	498.2
Wavelength(Å) Crystal system	0.71073 Triclinic	0.71073 monoclinic	1.54056 Orthorhombic	1.54056 Triclinic
Space group	Pī	*P*2(1)/*c*	*Pbca*	Pī
a(Å)	5.6934(3)	9.2066(7)	12.287 (5)	7.9981(5)
b(Å)	9.3416(5)	19.1090(13)	11.884 (5)	12.6314(8)
c(°)	12.6415(7)	18.589(2)	37.152 (5)	19.4346(10)
α(°)	116.513(6)	90	90	91.140(4)
β(°)	92.160(5)	100.46(3)	90	96.019(4)
γ(°)	102.669(5)	90	90	113.464(5)
Volume (Å^3)	3266.2(4)	3266.2(4)	5,425	856.46
(Calc.) density (g/cm^{-3})	1.557	1.557	1.543	1.701
2θ range Limiting indices Z *Rf* Temperature (K)	1.71–28.27 −16 ≤ h ≥ 6 −15 ≤ k ≥ 5 −15 ≤ l ≥ 5 2 0.0000842 298	1.71–28.27 −6 ≤ h ≥ 7 −34 ≤ k ≤ 34 −12 ≤ l ≥ 9 4 0.000018 298	10.25–67.27 0 ≤ h ≥ 15 0 ≤ k ≤ 15 0 ≤ l ≥ 47 8 0.0000323 298	12.56–68.00 −10 ≤ h ≥ 10 −12 ≤ k ≤ 12 −25 ≤ l ≥ 25 2 0.0000873 298

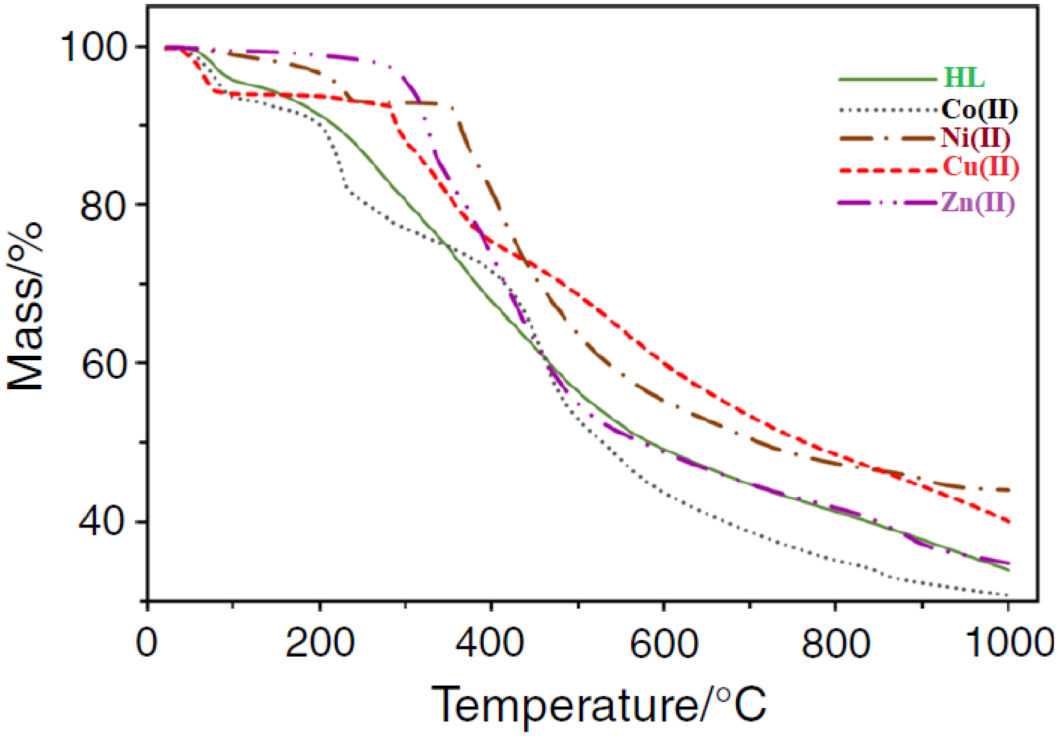

Figure 9. TGA spectra of 2-furan-2-ylmethyleneamino-phenyl-iminomethyl-phenol (HL) and its metal complexes (1-4).

Table 6. Thermal analyses data for 2-furan-2-ylmethyleneamino-phenyl-iminomethyl-phenol (HL) and their corresponding metal complexes (1–4)

Compound	Temp. range (°C)	Calc. mass loss (found) %	Assignment
HL	50–125	32.41 (32.38)	Loss of phenol
	125–205	23.45 (23.42)	Loss of furan
	205–395	37.23 (37.21)	Loss of $C_5H_4N_2O$
	395–999	12.40 (12.37)	Loss of carbon atoms
$[Co(L)(H_2O)Cl].2H_2O$	100–190	16.33 (15.31)	Loss of $2H_2O$(hydrated) + $1/2Cl_2$
	190–330	4.11 (4.08)	Loss of H_2O(coordinated)
	330–898	57.69 (57.94)	Loss of $C_{18}H_{13}N_2O$
	>900	17.11 (17.09)	CoO
$[Ni(L)(H_2O)Cl].4H_2O$	100–188	22.70 (22.68)	Loss of $4H_2O$(hydrated) + $1/2Cl_2$
	170–340	3.80 (3.78)	Loss of H_2O(coordinated)
	340–899	57.72 (57.69)	Loss of $C_{18}H_{13}N_2O$
	>900	15.77 (15.75)	NiO
$[Cu(L)(H_2O)Cl].3H_2O$	100–189	19.43 (19.41)	Loss of $3H_2O$(hydrated) + $1/2Cl_2$
	160–360	3.91 (3.87)	Loss of H_2O(coordinated)
	360–897	59.36 (59.32)	Loss of $C_{18}H_{13}N_2O$
	>900	17.26 (17.23)	CuO
$[Zn(L)(H_2O)Cl].5H_2O$	100–190	25.19 (25.16)	Loss of $5H_2O$(hydrated) + $1/2Cl_2$
	160–340	3.61 (3.57)	Loss of H_2O(coordinated)
	340–898	54.85 (54.82)	$C_{18}H_{13}N_2O$
	>900	16.33 (16.30)	ZnO

of the ligand ($C_5H_4N_2O$) (Found 37.21%, calc. 37.23%). The fourth stage in the temperature ranges 395–999°C corresponding to loss of carbon atoms (Found 22.1%, calc. 22.00%).

For Co(II), Ni(II), Cu(II) and Zn(II) complexes showed TG curves in the temperature range of ~100–190 °C loss of two, four, three and five hydrated water molecules+ 1/2 Cl_2 molecules. The second stage is related to loss of one molecule of coordinated water for metal (II) complexes (Co(II), Ni(II), Cu(II) and Zn(II)), respectively. The third stage is related to loss of the part of furan-Schiff's base ligand (HL). The final weight losses are due to the decomposition of the rest of the ligand and metal (II) oxide residue.

The kinetic and thermodynamic parameters (Table 7) of decomposition process have been calculated using Coats–Redfern (CR), Horowitz–Metzger (HM), and Piloyan–Novikova (PN) models[28–30]. From the results obtained, the following remarks can be pointed out:

(1) The energy of activation (E) values increases on going from one decomposition stage to another for a given complex, indicating that the rate of decomposition decreases in the same order. Generally stepwise stability constants decrease with an increase in the number of ligand attached to a metal ion. Conversely, during decomposition reaction the rate of removal of remaining ligands will be smaller after the expulsion of furan-Schiff's base ligand (HL)[31].

(2) The ΔG values increases significantly for the subsequently decomposition stages due to increasing the TΔS values from one stage to another. This may be attributed to the structural rigidity of the remaining complex after the expulsion of more ligands, as compared with the precedent complex, which require more energy, TΔS, for its rearrangement before undergoing any compositional change[26].

(3) The ΔS negative values for the decomposition steps indicate that all studied metal(II) complexes are more ordered in their activated states[27].

(4) The ΔH positive values mean that the decomposition processes are endothermic[31].

Table 7. Kinetic parameters of 2-furan-2-ylmethyleneamino-phenyl-iminomethyl-phenol (HL) and their corresponding metal(II) complexes

Compound	Decomposition temperature (°C)	Method	Parameters					Correlation coefficient
			E_a (kJ mol^{-1})	A (s^{-1})	ΔS□ (J mol^{-1} K^{-1})	ΔH□ (kJ mol^{-1})	ΔG□ (kJ mol^{-1})	
HL	122-447	CR	28.4	5.2	−247	24.2	164	0.9977
		HM	38.1	6.5	−235	33.3	169	0.9972
		PN	28.6	5.8	−241	31.8	165	0.9974
$[Co(L)(H_2O)Cl].2H_2O$	142–372	CR	38.9	162	−203	**54.2**	**162**	0.9924
		HM	42.3	163	−207	**55.6**	**165**	0.9928
		PN	41.7	162	−205	**56**	**163**	0.9929
$[Ni(L)(H_2O)Cl].4H_2O$	175–315	CR	62.9	172	−223	63.2	158	0.9897
		HM	63.2	173	−222	64.8	155	0.9895
		PN	62.7	174	−224	63.8	157	0.9898
$[Cu(L)(H_2O)Cl].3H_2O$	193–347	CR	68.8	180	−238	54.2	167	0.9896
		HM	68.3	182	−236	64.8	166	0.9899
		PN	69.1	179	−237	65.2	164	0.9897
$[Zn(L)(H_2O)Cl].5H_2O$	187–374	CR	66.6	169	−242	64.7	159	0.9887
		HM	67.2	170	−244	55.8	158	0.9888
		PN	66.8	171	−243	56.3	157	0.9885

Anticancer activity of HL ligand and complexes (1-4), upon studying the complete results, the ligand was observed to hinder the cell proliferation as compared to isolated metal(II) complexes having values of 24.82, 58.9, 62.7, 73.8 and 87.3% respectively in a 1000ppm concentration in contrast to the control cells which have not been treated cells. The anticancer screening data are compiled in Table 8. The molecular structures along with atom numbering electron density, and electrostatic potential of 2-furan-2-ylmethyleneamino-phenyl-iminomethyl-phenol (HL) and its isolated complexes are shown in Figures 10-14. Analysis of the data in Tables 9-11 calculated for the bond lengths and angles for the bond, one can conclude the following remarks:

- The actual bond angles ∠ and lengths are close to the optimal values, and thus the proposed structures of the compounds are acceptable.
- C(6)-N(7), C(9)-N(10) and N(10)-C(11) bond lengths of the furan-Schiff's base ligand were enlarged in complexes due to participation in coordination upon forming M-N(7) and M-N(10) bonds, where C(1)-O(5), C(4)-O(5) and C(13)-O(18) were mostly shortened and in some complexes enlarged upon coordination.
- The bond length O(18)-H(30) with the value 0.975 Å disappears upon coordination as the ligand acts in a mononegative tetradentate manner by losing this proton. Also the value of this bond angle ∠C(13)-O(18)-H(32) which is 108.184° ensures the SP^3 hybridization of the oxygen atom which is an optimal supposition.
- This ligand's bond angles ∠C(1)-O(5)-C(4), ∠C(6)-N(7)-C(8), ∠C(9)-N(10)-C(11), C(12)-C(13)-O(18) and ∠C(14)-C(13)-O(18) are reduced or increased upon complexation.
- New bond angles were formed between the ligand and metal ions as ∠O(5)-M(21)-N(7), ∠N(7)-M(21)-N(10) and ∠N(10)-M(21)-O(18) with different values ranges between (64.489°-136.574°). The geometric structure of the complexes is shown in Figure 15.

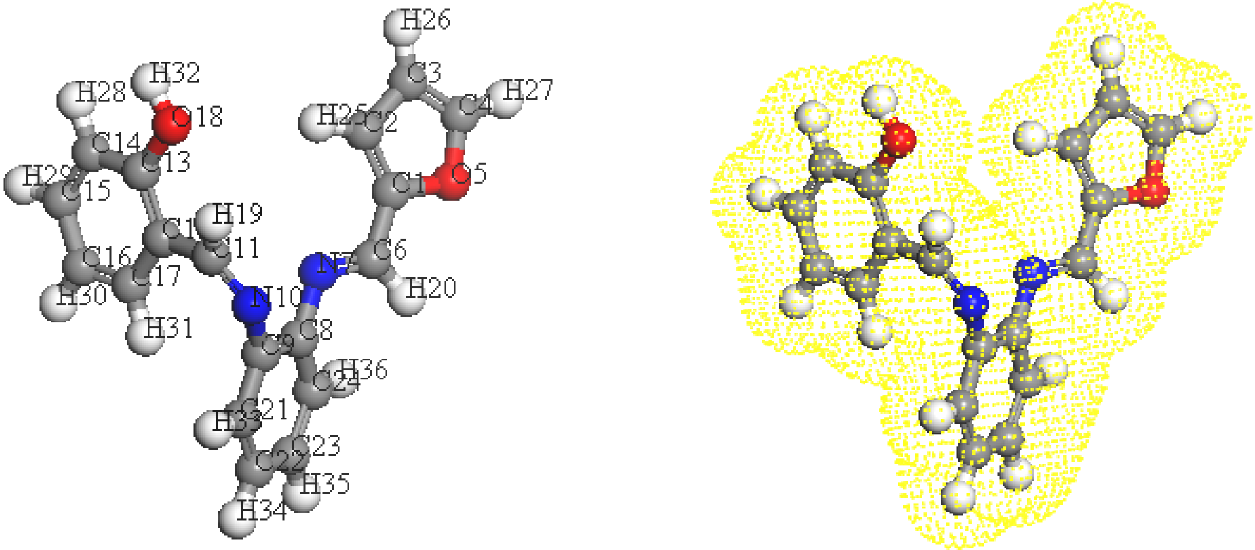

Molecular structure

Electron density

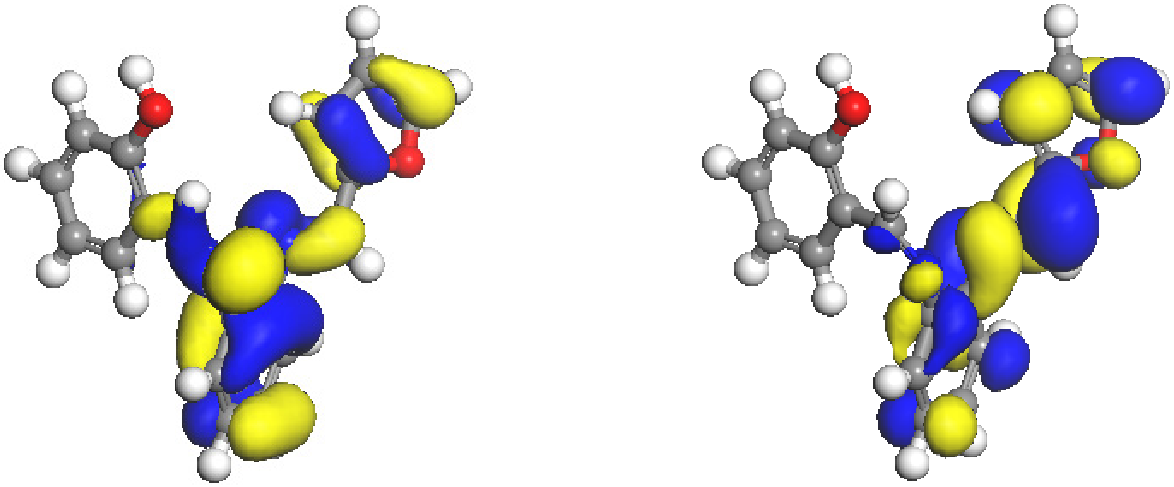

HOMO

LUMO

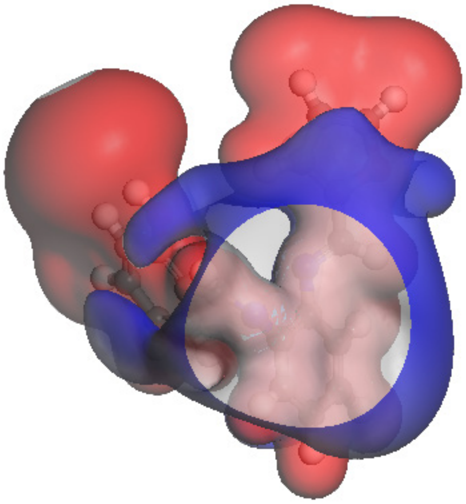

Electrostatic potential

Figure 10. The molecular structure, electron density, HOMO, LUMO and electrostatic potential of the ligand HL.

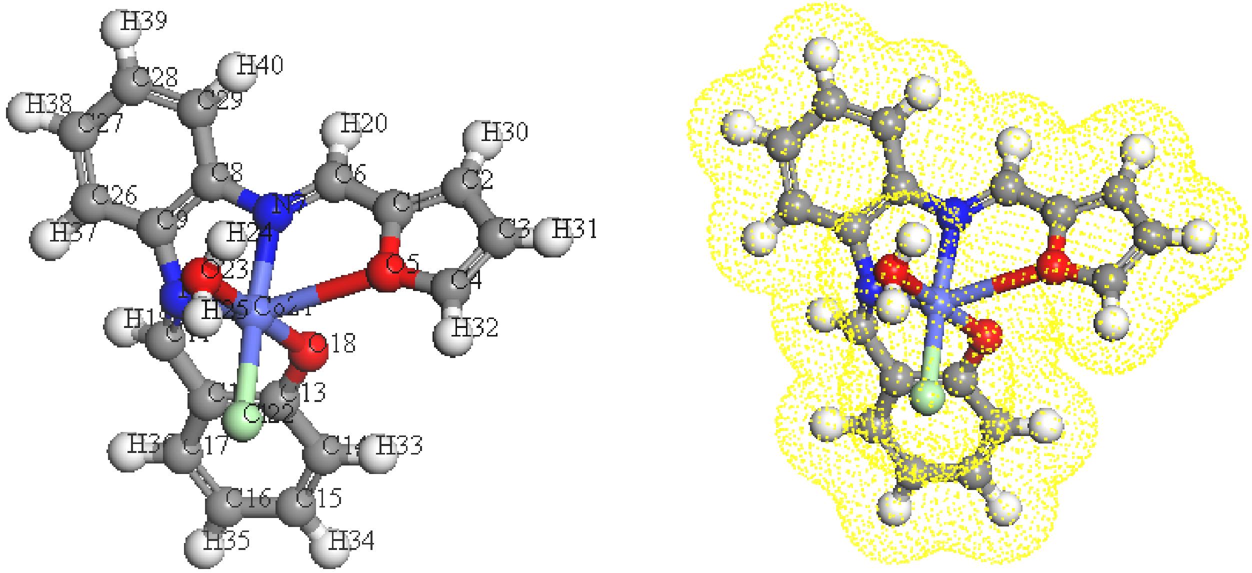

Molecular Structure

Electron density

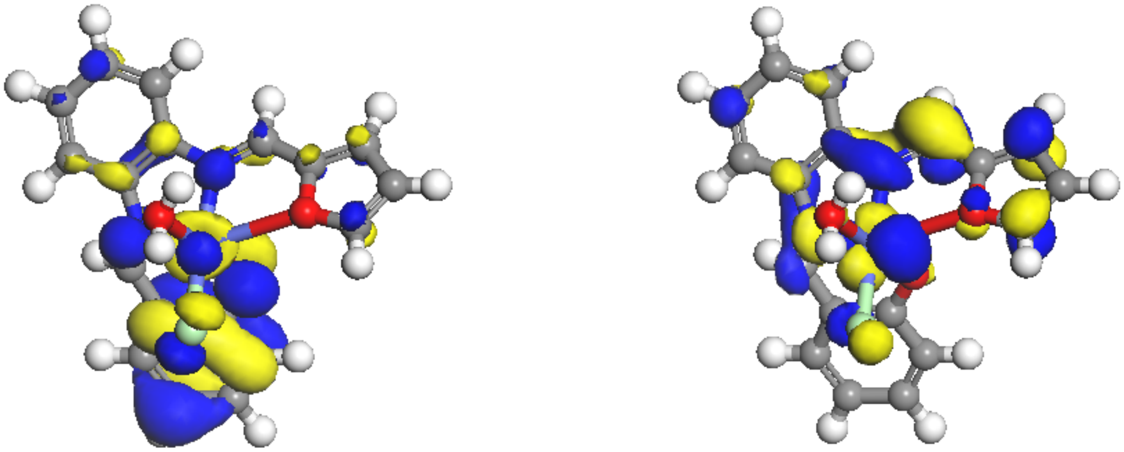

HOMO

LUMO

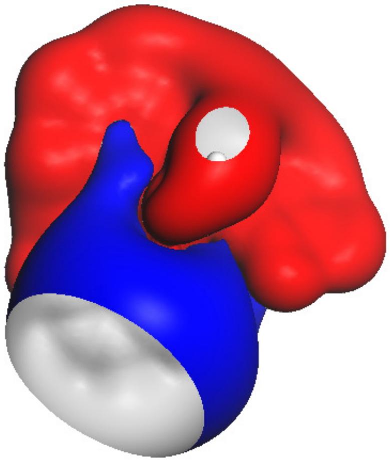

Electrostatic potential

Figure 11. The molecular structure, electron density, HOMO, LUMO and electrostatic potential of the Co^{II}-L complex.

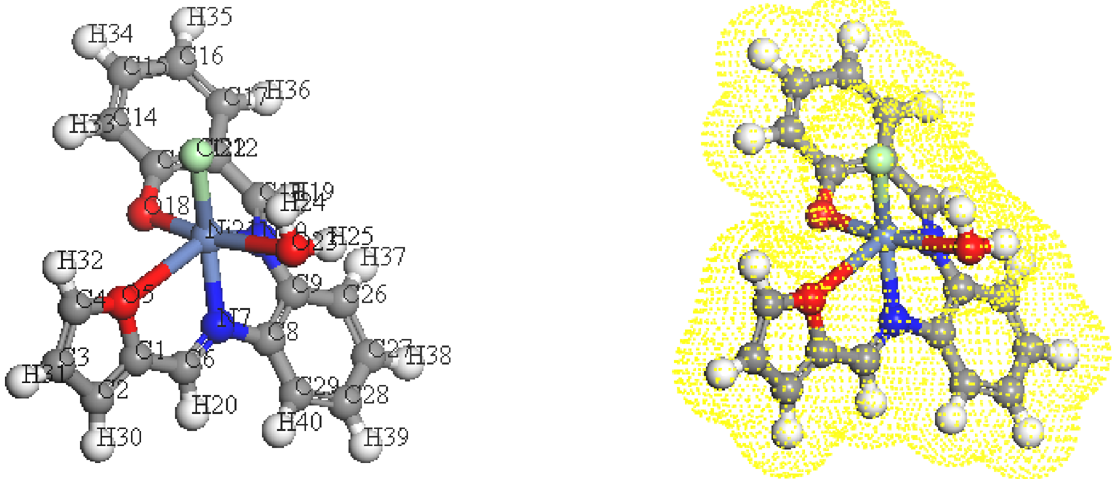

Molecular structure

Electron density

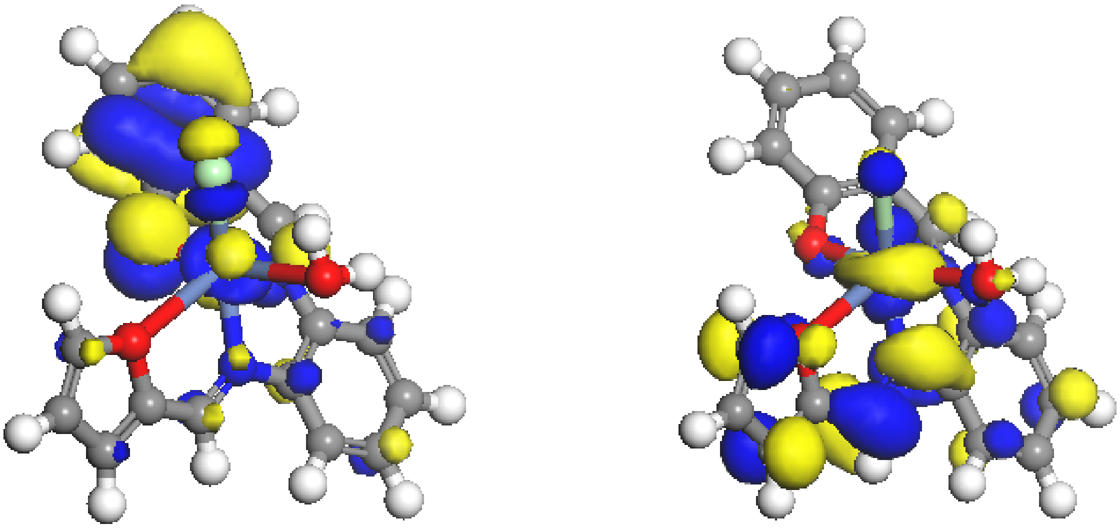

HOMO

LUMO

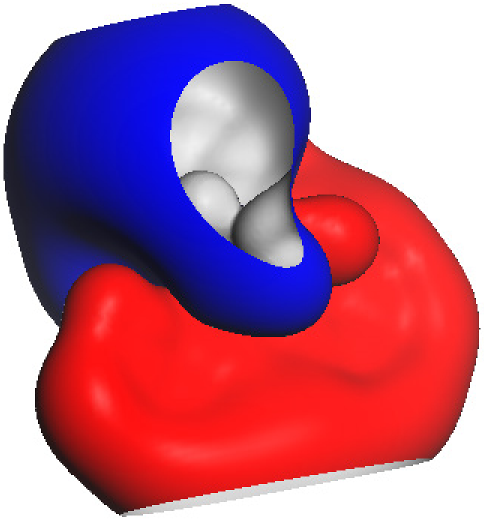

Electrostatic potential

Figure 12. The molecular structure, electron density, HOMO, LUMO and electrostatic potential of the Ni^{II} –L complex.

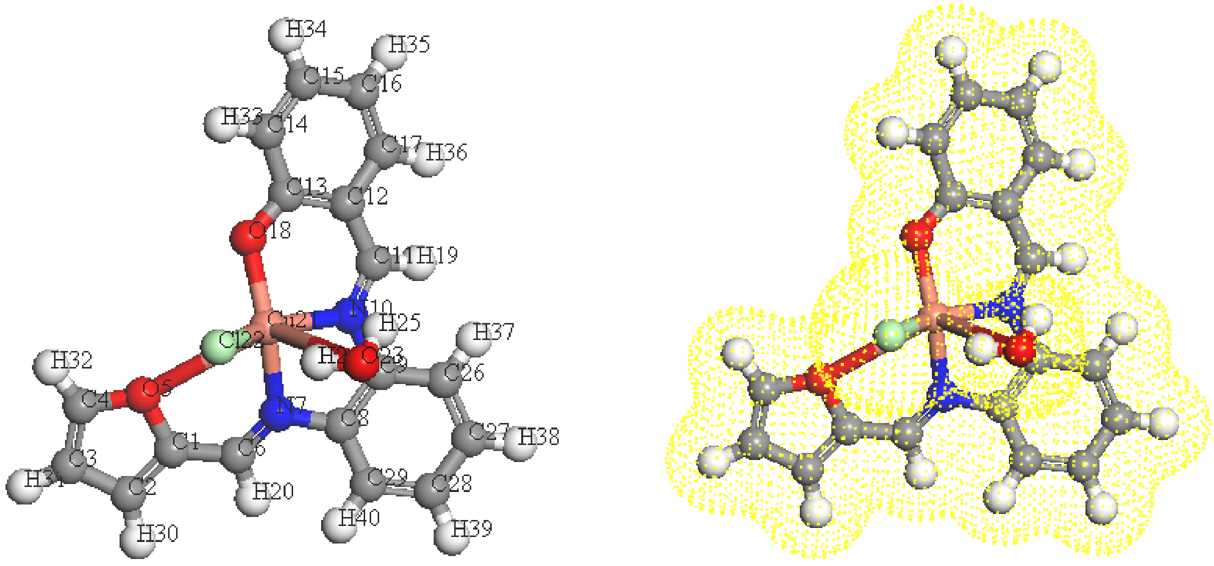

Molecular structure

Electron density

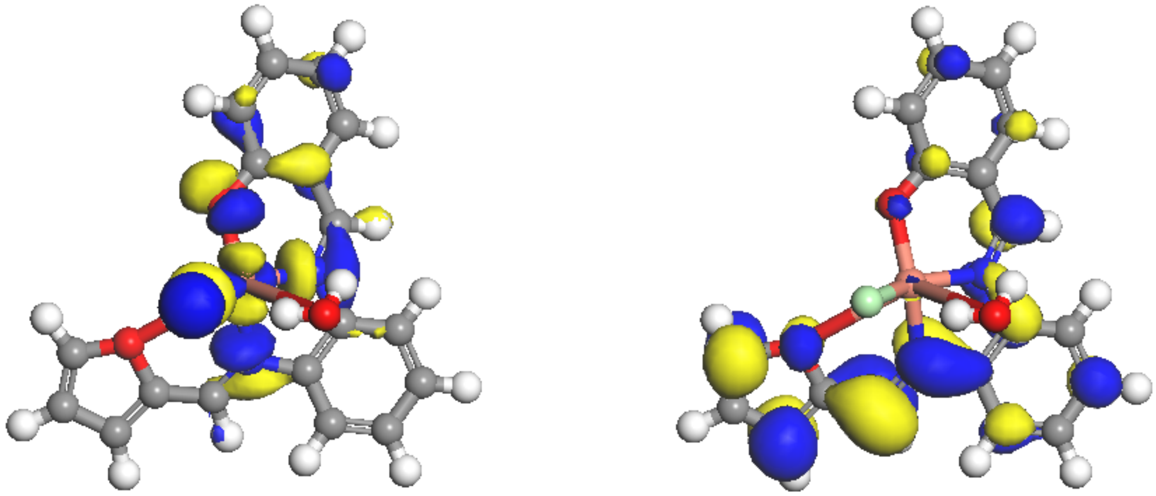

HOMO

LUMO

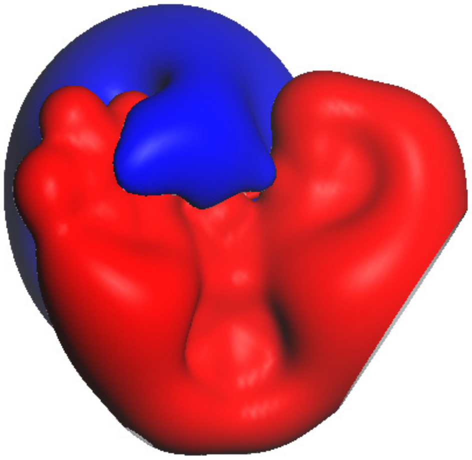

Electrostatic potential

Figure 13. The molecular structure, electron density, HOMO, LUMO and electrostatic potential of the Cu^{II}-L complex.

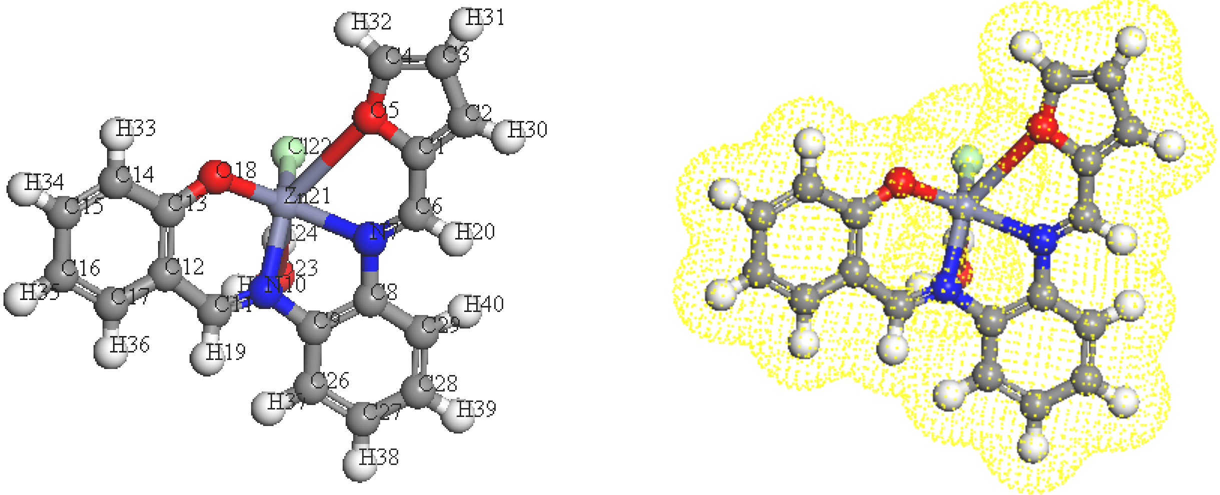

Molecular structure

Electron density

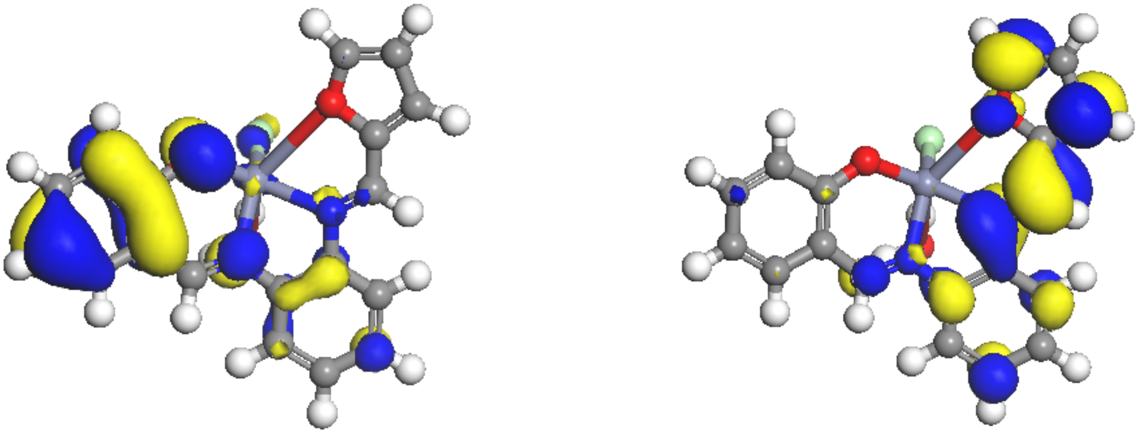

HOMO

LUMO

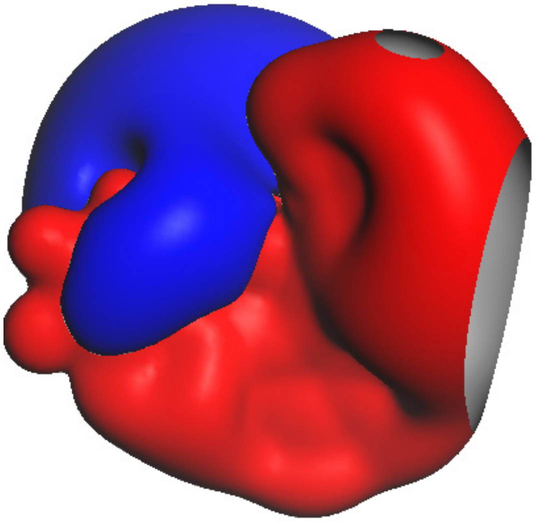

Electrostatic potential

Figure 14. The molecular structure, electron density, HOMO, LUMO and electrostatic potential of the Zn^{II}-L complex.

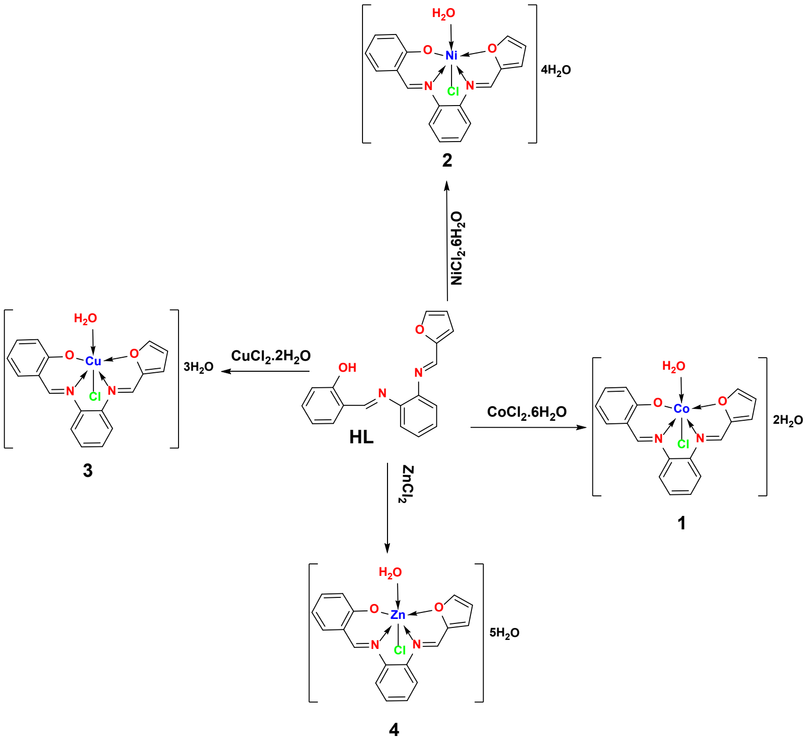

Figure 15. Synthesis of metal complexes Schiff base derived from HL with Co(II), Ni(II), Cu(II) and Zn(II) ions.

Table 8. Anticancer activity of furan-Schiff's base ligand (HL) and its corresponding metal(II) complexes (1-4)

Compound	Phytoextract concentrations (ppm)	*Cell viability (%)*
HL	Control	0±0.06
	100	0±0.35
	500	0±0.24
	1000	24.8±0.24
1	Control	0±0.23
	100	18.9±0.33
	500	23.7±0.24
	1000	58.9±0.07
2	Control	0±0.03
	100	15.8±0.23
	500	8.5±0.16
	1000	62.7±0.35
3	Control	0±0.06
	100	14.7±0.26
	500	13.4±0.23
	1000	73.8±0.13
4	Control	0±0.08
	100	27.5±0.26
	500	23.8±0.14
	1000	87.3±0.34

Table 9. Comparison between the bond lengths of the Schiff base ligand and its complexes

Bond length	Ligand	Co^{II} -L	Ni^{II} -L	Cu^{II}-L	Zn^{II}-L
C(1)-O(5)	1.394	1.393	1.388	1.386	1.389
C(4)-O(5)	1.372	1.377	1.369	1.368	1.370
C(6)-N(7)	1.299	1.329	1.313	1.312	1.311
N(7)-C(8)	1.408	1.408	1.425	1.424	1.421
C(9)-N(10)	1.412	1.415	1.410	1.415	1.411
N(10)-C(11)	1.292	1.314	1.313	1.314	1.311
C(13)-O(18)	1.377	1.325	1.316	1.312	1.321
O(18)-H(32)	0.975	--	--	--	--
O(5)-M(21)	--	2.825	2.945	3.191	2.999
N(7)-M(21)	--	2.020	2.056	2.058	2.148
N(10)-M(21)	--	1.950	2.015	1.998	2.057
O(18)-M(21)	--	1.893	2.020	1.973	2.998
M(21)-Cl(22)	--	2.328	2.233	2.300	2.276
M(21)-O(23)	--	2.068	2.599	3.855	4.202

Table 10. Comparison between the bond angles of the Schiff base ligand and its complexes

Bond angle	Ligand	Co^{II} -L	Ni^{II} -L	Cu^{II}-L	Zn^{II}-L
C(1)-O(5)-C(4)	106.638	107.075	106.819	106.519	106.590
C(6)-N(7)-C(8)	120.263	123.365	120.804	120.060	121.256
C(9)-N(10)-C(11)	125.101	123.951	124.926	123.265	124.319
C(12)-C(13)-O(18)	118.139	123.559	123.813	124.776	125.670
C(14)-C(13)-O(18)	121.222	118.554	119.444	118.094	117.790
C(13)-O(18)-H(32)	108.184	--	--	--	--
O(5)-M(21)-N(7)	--	68.315	67.236	60.015	65.011
N(7)-M(21)-N(10)	--	81.157	80.703	81.108	136.574
N(10)-M(21)-O(18)	--	89.319	86.354	90.197	93.233
C(5)-M(21)-O(18)		81.460	90.483	105.611	95.796

Table 11. Some energetic data containing total energy, binding energy, dipole moment, HOMO, LUMO,ΔE_{Gap} and electrostatic potential

Compd	Total Energy (kcal/mol)	Binding energy (kcal/mol)	Dipole moment (D)	HOMO (ev)	LUMO (ev)	ΔE_{Gap}	Electrostatic potential (kcal/mol)
ligand	-5.99×10^5	−4285.551	6.1027	−4.863	−2.454	2.411	−1160.707
Co^{II} -L	1.040×10^6	−4659.968	9.3964	−4.978	−3.398	1.58	−3539.32
Ni^{II} -L	-1.057×10^6	−4651.276	10.9206	−4.931	−3.413	1.518	−3319.623
Cu^{II}-L	-1.075×10^6	−4585.814	12.6023	−4.700	−3.322	1.378	−1001.360
Zn^{II}-L	-1.095×10^6	−4561.082	11.1595	−5.206	−3.326	1.88	−1731.549

4. Reference

1. Kim MS. Future cancer therapy with molecularly targeted therapeutics challenges and strategies. Biomolecules and the raputics. 2011; 19(4):371–9. Crossref.
2. Therrien B. Transporting and shielding photosensitisers by using water-soluble organometallic cages a new strategy in drug delivery and photodynamic therapy. Chemistry A European Journal. 2013; 19(26):8378–683. Crossref. PMid:23737435
3. Smith GS, Therrien B. Targeted and multifunctional arene ruthenium chemotherapeutics. Dalton Transactions. 2011; 40(41):10793–800. Crossref. PMid:21858344
4. Jungwirth U, Kowol CR, Keppler BK, Hartinger CG, Berger W, Heffeter P. Anticancer activity of metal complexes involvement of redox processes. Antioxidant Redox Signaling. 2011; 15(4):1085–127. Crossref. PMid:21275772 PMCid:PMC3371750
5. Mao J, Zhang Y, Zhu J, Zhang C, Guo Z. Molecular combo of photodynamic therapeutic agent silicon(iv) phthalocyanine and anticancer drug cisplatin. Chemical Communications. 2009; 28(8):908–10. Crossref. PMid:19214312
6. Terenzi A, Lotsch D, Schoonhoven S, Roller A, Kowol CR, Berger W, Keppler BK, Barone G. Another step toward DNA selective targeting Ni(II) and Cu(II) complexes of a Schiff base ligand able to bind gene promoter G-quadruplexes. Dalton Transactions. 2016; 45(18):7758–67. Crossref. PMid:27054617 PMCid:PMC5048337
7. Hazra S, Paul A, Sharma G, Koch B, Da Silva MF, Pombeiro AJL. Sulfonated Schiff base Sn(IV) complexes as potential anticancer agents. Journal of Inorganic Biochemistry. 2016; 162:83–95. Crossref. PMid:27338202
8. Metcalfe C, Thomas JA. Kinetically inert transition metal complexes that reversibly bind to DNA. Chemical Society Reviews. 2003; 32(4):215–43. Crossref. PMid:12875027
9. Anna VR, Prasad KT, Wang P, Rao KM. Study of half-sandwich mono and dinuclear complexes of platinum group metals containing pyrazolyl pyridine analogues Synthesis and spectral characterization. Journal of Chemical Sciences. 2012; 124(3):565–75. Crossref.
10. Arturo S, Giampaolo B, Giuseppe R, Maria LG, Salvatore T. The interaction of native DNA with iron(III)-N, N'-ethylene-bis(salicylideneiminato)-chloride. Journal of Inorganic Biochemistry. 2004; 98(4):589–94. Crossref PMid:15041238
11. Lei K, Liu W, Huang X, Wand D. Synthesis. Crystal structure and DNA-binding study on the trinitrate{2,2'-[2,3-naphthylenebis(oxy)]-bis(N,Ndiisopropyl(acetamide))} Gadolinium(III) Complex. Chemical Pharmaceutical Bulletin. 2006; 54(10):1150–4. Crossref. PMid:16880660
12. Utthra PP, Pravin N, Raman N. Scrutinizing the DNA damaging and antimicrobial abilities of triazole appended metal complexes. Journal of Photochemistry and Photobiology B Biology. 2016; 158(3):136–44. Crossref. PMid:26971279
13. Saghatforoush LA, Valencia L, Chalabian F, Ghammamy S. Synthesis Characterization crystal structure and biological studies of a cadmium(ii) complex with a tridentate ligand 4′-Chloro-2,2′:6′,2″-terpyridine. Bioinorganic Chemistry and Applications. 2011; 2011:1–7. Crossref. PMid:21738495 PMCid:PMC3119424
14. Mahendiran D, Kumar RS, Viswanathan V, Velmurugan D, Kalilur D, Rahiman AK. Targeting of DNA molecules BSA/c-Met tyrosine kinase receptors and anti proliferative activity of bis(terpyridine)copper(II) complexes. Dalton Transactions. 2016; 45:7794–814. Crossref. PMid:27063595
15. Marmur J. A procedure for the isolation of deoxyribonucleic acid from micro-organisms. Journal of Molecular Biology. 1961; 3(2):208–18. Crossref.
16. Tan LF, Wang F, Chao H, Weng C. Ruthenium(II) mixed-ligand complex containing 2-(4'-benzyloxy-phenyl) imidazo[4,5-f][1,10]phenanthroline synthesis DNA-binding and photocleavage studies. Journal of Inorganic Biochemistry. 2007; 101(4):700–8. Crossref. PMid:17316812
17. Patel BK, Govin SJ, Liebman SW. The yeast global transcriptional co-repressor protein Cyc8 can propagate as a prion. Nature Cell Biology. 2009; 11(3):344–9. Crossref. PMid:19219034 PMCid:PMC2667906
18. Ammar RAA, Alaghaz AN, Zayed MEA, Al-Bedair LA. Synthesis spectroscopic molecular structure antioxidant antimicrobial and antitumor behavior of Mn(II), Co(II), Ni(II), Cu(II) and Zn(II) complexes of O2N type tridentate chromone-2-carboxaldehyde Schiff's base ligand. Journal of Molecular Structure. 2017; 1141:368–81. Crossref.
19. Nakamoto K. Infrared Raman spectra of Inorganic and Coordination Compounds, Part-B, 5th ed. New York: Wiely Interscience Publications; 1997. p. 1–432. PMid:9192079
20. Salman RD, Farrant RD, Lindon JC. Studies of tautomerism in 2 hydroxynaphthaldehyde schiff bases by multinuclear magnetic resonance. Spectroscopy Letters. 1991; 24(9):1071–8. Crossref.
21. Devi J, Batra N, Malhotra R. Ligational behavior of Schiff bases towards transition metal ion and metalation effect on their antibacterial activity. Spectrochimica Acta Part A Molecular and Biomolecular Spectroscopy. 2012; 97(3):397–405. Crossref. PMid:22813991
22. Keskioglu E, Gunduzalp AB, Cete S, Hamurcu F, Erk B. Cr(III), Fe(III) and Co(III) complexes of tetradentate (ONNO) Schiff base ligands synthesis characterization properties and biological activity. Spectrochimica Acta Part A Molecular and Biomolecular Spectroscopy. 2008, 70(3):634–40. Crossref. PMid:17904895

23. Alaghaz AMA, Ammar YA, Bayoumi HA, Aldhlmani SA. Synthesis spectral characterization thermal analysis molecular modeling and antimicrobial activity of new potentially N2O2 azo-dye Schiff base complexes. Journal of Molecular Structure. 2014; 1074:359–75. Crossref.
24. Alaghaz AN, Ammar RA. New dimeric cyclodiphosph(V) azane complexes of Cr(III), Co(II), Ni(II), Cu(II), and Zn(II) preparation characterization and biological activity studies. European Journal of Medicinal Chemistry. 2010; 45(4):1314–22. Crossref. PMid:20089330
25. Jorgensen CK. Complexes of the 4d- and 5d-Groups I crystal field spectra of rhodium(III) and iridium(III). Acta Chemica Scandinavica. 1956; 10(2):500–17. Crossref.
26. Alaghaz AMA, Zayed ME, Alharbi SA, Ammar RAA, Elhenawy A. Synthesis characterization biological activity molecular modeling and docking studies of complexes 4-(4-hydroxy)-3-(2-pyrazine-2-carbonyl) hydrazonomethylphenyl-diazen-yl benzenesulfon-amide with manganese(II), cobalt(II), nickel(II), zinc(II) and cadmium(II). Journal of Molecular Structure. 2015; 1084:352–67. Crossref.
27. Alaghaz AMA, Zayed ME, Alharbi SA. Synthesis spectral characterization molecular modeling and antimicrobial studies of tridentate azo-dye Schiff base metal complexes. Journal of Molecular Structure. 2015; 1084:36–45. Crossref.
28. Coats AW, Redfern JP. Kinetic parameters from thermogravimetric data. Nature. 1964; 201:68–9. Crossref.
29. Horowitz HH, Metzger G. A New analysis of thermogravimetric traces. Analytical Chemistry. 1963; 35(10):1464–8. Crossref.
30. Piloyan GO, Pyabonikar ID, Novikova OS. Determination of activation energies of chemical reactions by differential thermal analysis. Nature. 1966; 212:1229–304. Crossref.
31. El-Gammal OA. Synthesis characterization molecular modeling and antimicrobial activity of 2-(2-(ethylcarbamothioyl) hydrazinyl)-2-oxo-N-phenylacetamide copper complexes. Spectrochimica Acta Part A Molecular and Biomolecular Spectroscopy. 2010; 75(2):533–42. Crossref. PMid:20036192